Viscoelastic Behavior of Cellulose Acetate in a Mixed Solvent System

Collins Appaw,[†] Richard D. Gilbert,[‡] and Saad A. Khan*[,†]

Departments of Chemical and Biomolecular Engineering and Wood and Paper Science, North Carolina State University, Raleigh, North Carolina 27695

John F. Kadla*

Advanced Biomaterials Chemistry, Faculty of Forestry, University of British Columbia, Vancouver, BC V6T 1Z4 Canada

Received December 9, 2006; Revised Manuscript Received March 8, 2007

The effect of increasing water composition on the rheological and microstructural behavior of a ternary cellulose acetate (CA)/*N*,*N*-dimethylacetamide (DMA)/water system is examined. Addition of water to the CA/DMA system results in enhanced steady shear viscosity and dynamic viscoelastic properties and ultimately to phase-separated gel formation. The changes in dynamic rheological behavior of the system during gelation correlate well with the combined solubility parameter (δ) and, in particular, the Hansen hydrogen-bonding solubility parameter index (δ_h) of the solvent system, suggesting hydrogen-bonding interactions may be the major route initiating the sol−gel process. For all gels studied, the elastic modulus and the critical stress to yield shifts to higher values with increasing CA concentration and/or water content. In addition, the elastic modulus exhibits a power-law behavior with water content, with the same power-law exponent observed for gels containing different CA concentrations. Addition of water leads to formation of a denser gel network, as evidenced from direct visualization of the gel microstructure through confocal microscopy.

Introduction

Cellulose and its derivatives are some of the most widely utilized natural materials. Cellulose is a linear homopolymer consisting of β (1−4)-linked anhydroglucopyranose units (AGU).[1] Extensive intra- and intermolecular hydrogen bonding make cellulose insoluble in most common organic solvents.[2,3] As a result, cellulose is typically derivatized[4] to facilitate dissolution and processing.

Cellulose acetates (CA) are cellulose esters[5] that are partially substituted at the C-2, 3-, and 6-positions of the AGU.[4,6,7] The solubility of CA in various solvents is dependent on a number of factors including the degree of substitution (DS)[6,8] and the hydrogen-bonding component of the solubility parameter index (δ_h) of the solvent.[9] Acetylation disrupts the intra- and intermolecular interactions within the cellulose molecule enabling interaction with the solvent;[6] basic solvents interact primarily with the hydroxyl groups, whereas acidic solvents interact with the acetyl groups.[10] Cellulose acetates with a DS between 0.5 and 1 are soluble in aqueous solutions,[11,12] whereas those with DS >1 tend to be insoluble in aqueous medium but soluble in many organic solvent systems. Cellulose acetate molecules are never completely molecularly dispersed in solution,[6] rather existing as complex molecular associates, the extent of which depends on the strength and amount of the intra- and intermolecular interactions (e.g., hydrogen bonding). For example, *N*,*N*-dimethylacetamide (DMA), which readily dissolves CA of DS ranging from 0.49 to 2.92[6] shows evidence of aggregates or associates of CA molecules even in dilute solution, the result of long-range hydrogen bond interactions between DMA and CA.[6,8]

Cellulose acetates are extensively used in filtration/membrane[13,14] and encapsulation[15] applications. In such systems sophisticated network structures are required. This is typically achieved through aggregation-induced phase separation.[16,17] In polymeric systems phase separation can be induced by solvent evaporation, changes in temperature, or the addition of a nonsolvent.[18] In nonsolvent-induced phase separation, the concentration of polymer, solvent, and nonsolvent are critical.[19,20] Depending on the system and component concentrations, phase separation can lead to physical gel formation.[21] Gelation occurs as a result of nonsolvent-induced polymer aggregation and the formation of large macromolecular associates and clusters.[22,23] Depending on the solvent system, CA will exhibit varying solution properties, where the sol−gel transition and gel behavior will be influenced by the interactions between the CA/solvent/nonsolvent. Nonsolvent phase-separated gelation has been observed in several CA systems including dioxane/water[24] and ethanol/water[25] mixtures.

Extensive research has been conducted into the associative behavior of CA in numerous solvent systems. However, very little has been reported on concentrated CA solutions, and to our knowledge no systematic studies have been undertaken in understanding the rheology and gelation of CA in mixed solvent systems. In this study, we investigate the sol−gel behavior of a semiconcentrated ternary system comprising CA, DMA, and water. Specifically, we examine the characteristics leading to gelation by nonsolvent (water) addition using steady shear and dynamic rheological measurements.[26] Our results indicate that increasing water content in the ternary system leads to changes in the viscoelastic behavior and ultimately to phase-separated

* Corresponding authors. Phone: 604 827-5254 (J.F.K.); 919 515-4519 (S.A.K.). Fax: 604 822-9104 (J.F.K.); 919 515-3465 (S.A.K.) E-mail: john.kadla@ubc.ca (J.F.K.); khan@eos.ncsu.edu (S.A.K.).

[†] Department of Chemical and Biomolecular Engineering.

[‡] Department of Wood and Paper Science.

10.1021/bm0611681 CCC: $37.00
Published on Web 04/26/2007

gel formation. The elastic modulus of the gels correlates well with the combined solubility parameter (δ) and, in particular, the Hansen hydrogen-bonding solubility parameter index (δ_h) of the solvent system, suggesting hydrogen-bonding interactions may be the major route initiating the sol−gel process. The rheological experiments are supplemented with confocal scanning laser microscopy (CSLM) to directly probe gel microstructure.

Experimental Section

Materials. *N*,*N*-Dimethylacetamide (DMA, HPLC grade) and cellulose acetate (CA, M_n ca. 50 000 g/mol, degree of acetylation (DA) = 2.44 (39.7 wt % acetyl content)) were purchased from Sigma-Aldrich and used as received. Deionized water was utilized as the nonsolvent.

Sample Preparation. All samples were prepared from a bulk 20 wt % CA in DMA solution. The specific CA/DMA/water concentrations used in this study were obtained by adding appropriate amounts of DMA and deionized water to the 20 wt % CA/DMA solution. The samples were mechanically mixed and conditioned for 24 h at 25 °C. The samples were then blanketed with nitrogen and heated to 70 °C for 10 min to ensure complete miscibility and left at ~25 °C for at least a 5 days prior analysis. All stock solutions and dilutions were prepared on a weight basis.

Rheological Measurements. Steady and dynamic rheological experiments were conducted with an AR 2000 rheometer (TA Instruments, New Castle, DE) using either a cone and plate or parallel plate geometry. All experiments were performed at 25 °C. In the dynamic experiments, the samples were subjected to a sinusoidal deformation as both a function of increasing strain amplitude or frequency of oscillation, and the corresponding elastic (G') and viscous (G'') moduli were measured.[26−28] Dynamic stress sweep experiments were performed to determine the linear viscoelastic (LVE) regime prior to the frequency sweep experiments. Parallel plate geometry was used for the gels. Experiments were repeated with serrated plates to check for slippage, and results showed no evidence of such occurrence.

Cloud Point. Cloud point studies were performed using an Edmunds JDS uniphase helium−neon laser light source operating at a maximum voltage output of 5 mV.[29] The procedure involved passing a laser source through the sample and the subsequent recording of the transmitted output intensity on an Edmunds PD200 laser meter. Measurements were made using a quartz cuvette having an optical path length of 1 cm. For high-viscosity samples, such as gels, a spatula was used to carefully transfer the sample into the cuvette.

Confocal Scanning Laser Microscopy (CSLM). A confocal scanning laser system (Leica TCS SP) attached to an inverted microscope (Leica DM IBRE, Leica Microsystems, Wetzlar, Germany) was used to obtain confocal images of the gel microstructure. Calcofluor white (0.01%, Aldrich) was used as the fluorescent dye, and samples were prepared as per the rheological experiments. The mixed samples were placed onto a microscope slide with a 0.12 mm thick spacer and covered with a glass cover. The samples were heated to 70 °C for 10 min and left at ~25 °C for at least a 5 days prior analysis. All images were viewed with a 100× numerical aperture 1.4 oil immersion objective lens.

Data Analysis. Samples for rheological analysis were run in duplicate, and results were within an error of 10%. In the CSLM experiments image analysis was done using Adobe Photoshop 7.0 (Adobe Systems Inc.). In the determination of the fractal dimension from CSLM, five layers through the sample thickness were analyzed by Image J software using the fractal box count method. Average fractal dimension and standard deviation were obtained.

Results and Discussion

Solution Rheology. The effect of nonsolvent (water) addition on the viscosity of the CA/DMA system was investigated using steady-state rheology. Figure 1A shows the viscosity profiles for a 10 wt % CA solution with different water content. At low water content, the viscosity exhibits a large Newtonian plateau followed by a power-law regime. With increasing water the viscosity curves change exhibiting high viscosity at low shear rates and the gradual disappearance of the zero-shear viscosity plateau. The disappearance of the Newtonian plateau at low shear rates suggests development of microstructure as water content is increased.

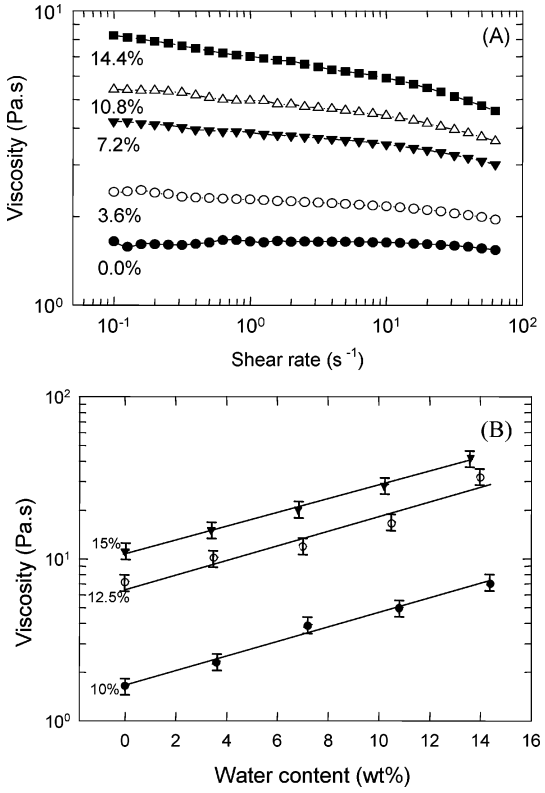

Figure 1. (A) Effect of water content on steady shear viscosity for a 10 wt % CA/DMA/water system and (B) viscosity as a function of water content obtained at shear rate of 1 s^{-1} for CA concentrations of 10 (●), 12.5 (○), and 15 (▼) wt %.

The effects of water content and CA concentration is illustrated more clearly in Figure 1B, which shows the low-shear viscosity as a function of water content for three different samples with different CA content. We find the viscosity to increase by almost an order of magnitude when the CA concentration is increased from 10 to 15 wt %. We also find the low-shear viscosity to increase exponentially with increased water content, with the exponent being same for all three CA concentrations studied. Further increase in water content leads to an opaque self-supporting gel-like material, as seen in Figure 2.

Gelation Characteristics. To quantify the sol−gel behavior of the CA ternary system the elastic (G') and viscous (G'') moduli are plotted as a function of frequency. Figure 2 illustrates the frequency behavior of G' and G'' at two different water contents for 10 wt % (Figure 2A) and 15 wt % (Figure 2B) CA concentrations. At low water content G'' is larger than G' for both CA concentrations, and the samples are transparent (shown only for one concentration). Both G' and G'' exhibit strong frequency dependence reminiscent of a polymer solution. At high water content G' and G'' increase by several orders of magnitude, and the sample resembles an opaque self-supporting material. The G' is larger than G'' over the entire frequency range studied, with both G' and G'' being relatively frequency

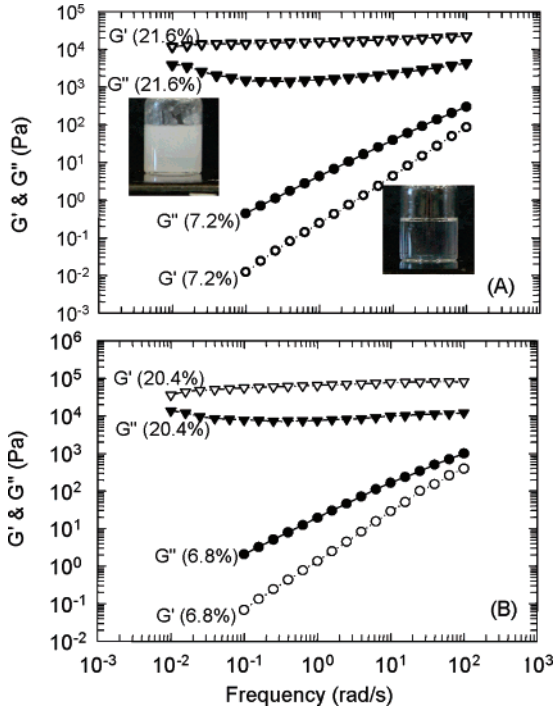

Figure 2. Viscous (G'') and elastic (G') moduli for (A) 10 wt % and (B) 15 wt % CA concentrations at low and high water content. Water contents are shown in brackets. The transition of a clear solution to an opaque self-supporting gel is shown for the 10 wt % CA sample.

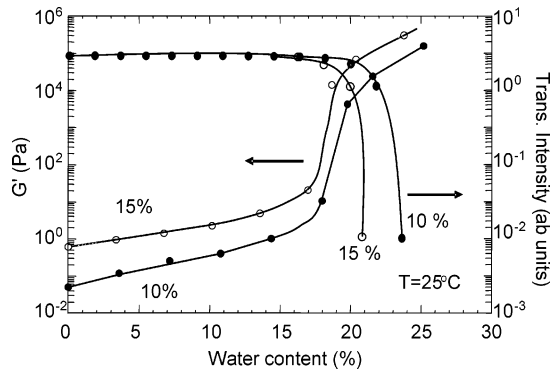

Figure 3. Effect of water content on transmission intensity and elastic moduli (G') for 10 and 15 wt % CA (1 rad s^{-1}).

independent, both features characteristic of a three-dimensional elastic gel.[30−32] Increasing the CA concentration from 10 to 15 wt % increases the magnitude of both G' and G'' at both high and low water contents.

Figure 3 illustrates the effect of water content on G' and cloud point. The elastic modulus, G', increases by over 4 orders of magnitude as the water content increases from 0 to 25 wt % for both the 10 and 15 wt % CA samples. Interestingly, curves for both CA concentrations show the same sigmoidal shape, with the 15 wt % CA system exhibiting a higher value, inline with the earlier viscosity observations (Figure 1B). As such, three distinct regimes exist in terms of G' enhancement: an initial region of slow G' increase with increasing water content, an intermediate regime of sharp G' increase with concomitant gel formation, followed once again by a slow increase in G'. The sharp increase in G' corresponds well with the sharp drop in transmission intensity. Analogous to G', increasing the CA concentration from 10 to 15 wt % results in the cloud point shifting to lower water content. Thus, an increase in CA concentration leads to gel formation at a lower water content

Table 1. Hansen Solubility Parameters for Cellulose Acetate, DMA, and Water at 25 °C[a,b]

	solubility parameters ($MPa^{1/2}$)			
	δ	δ_d	δ_p	δ_h
CA	25.1	18.6	12.7	11.0
DMA	22.7	16.8	11.5	10.2
water	48.0	15.5	16.0	42.4

[a] Ref 34. [b] δ_p, permanent dipole−dipole; δ_h, hydrogen bonding.

as polymer−polymer and polymer−nonsolvent interactions are more pronounced.

It is interesting to note that even in the water content range in which transmission remains constant, G' continues to increase with the addition of water indicating the sensitivity of rheological measurements. The increase in G' may be due to enhanced intermolecular interactions (e.g., hydrogen bonding) between CA−DMA−water. In solution, the hydroxyl (OH) groups on CA likely interact with the carbonyl group in DMA, analogous to the CA−acetone system.[33] With the addition of water new hydrogen bonds are established between water and DMA and to a much lesser extent CA. The result is an intensification of the hydrogen-bonding interactions in solution resulting in the observed increase in viscosity and G'. This complex hydrogen-bonding network system is further magnified by increasing the CA concentration from 10 to 15 wt %.

Solution property and phase behavior of polymers is very much dependent on intermolecular interactions of solvent(s) and solute, which must be overcome for dissolution. As the strength of intermolecular forces is equal to the cohesive energy density (CED), CED values can be used to predict solubility and solution behavior. Typically, Hildebrand solubility parameters (δ), which are the square root of CED, are used.[34] For mixtures, the solubility parameter is often taken as the sum of the products of the component solubility parameters and their volume fractions (ϕ):

$$\delta_{mix} = \sum_i \delta_i \phi_i$$

Accordingly, the addition of water to DMA leads to an increase in the solvent/nonsolvent solubility parameter (Table 1). Figure 4A illustrates G' as a function of solvent solubility parameter (δ). Both 15 and 10 wt % CA systems show a weak dependence on δ at low water content followed by a sharp increase in G' during the onset of the sol−gel transition, which is 2−3 $MPa^{1/2}$ higher than the solubility parameter of CA.

For polar systems the free energy change in mixing is dominated by hydrogen-bonding forces between various groups in the polymer and solvent.[34,35] Complete miscibility is expected to occur if the solubility parameters and degree of hydrogen bonding is similar between the components. As such a three-term set representing different contributions to the free energy of mixing, i.e., dispersive (δ_d), permanent dipole−dipole (δ_p), and hydrogen-bonding (δ_h) interactions, is widely utilized,[35] where

$$\delta^2 = \delta_d^2 + \delta_p^2 + \delta_h^2$$

Table 1 lists values of these terms for water, DMA, and CA. Although not completely accurate for every system, these parameters give improved agreement between δ and experi-

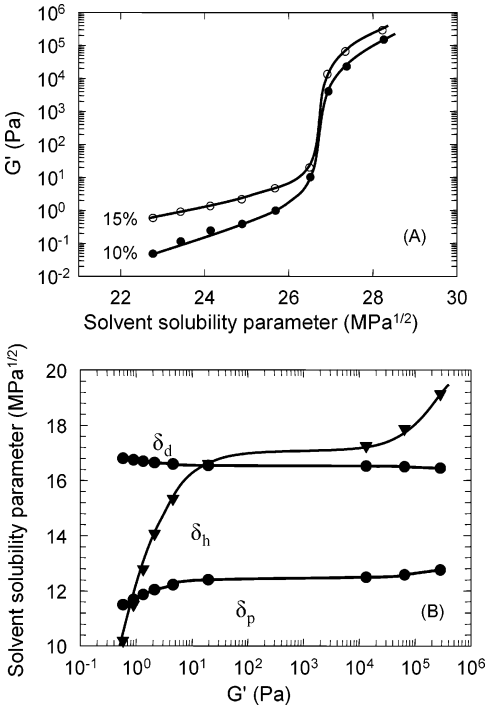

Figure 4. Effect of (A) solvent solubility parameter on elastic modulus G' at 10 and 15 wt % CA concentrations and (B) the influence of the individual solubility parameter index on G' (10 wt % CA) at a fixed frequency (1 rad s^{-1}).

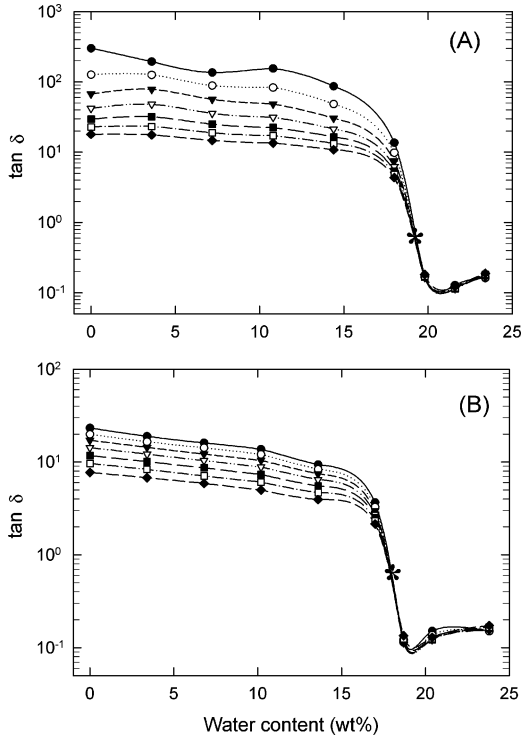

Figure 5. Multifrequency plot of tan δ as function of water content for (A) 10 wt % and (B) 15 wt % CA concentrations (● 0.631, ○ 1.00, ▼ 1.58, ▽ 2.50, ■ 3.90, □ 6.30, and ◆ 10.0 rad s^{-1}). The ∗ indicates the gel point.

mental data. The impact of the different solubility parameter components on G' are shown in Figure 4B. The hydrogen-bonding solubility parameter index (δ_h) is significantly affected, whereas both δ_d and δ_p remain relatively constant. This would seem to indicate that hydrogen-bonding interactions may be the major route initiating the sol−gel process in this system.

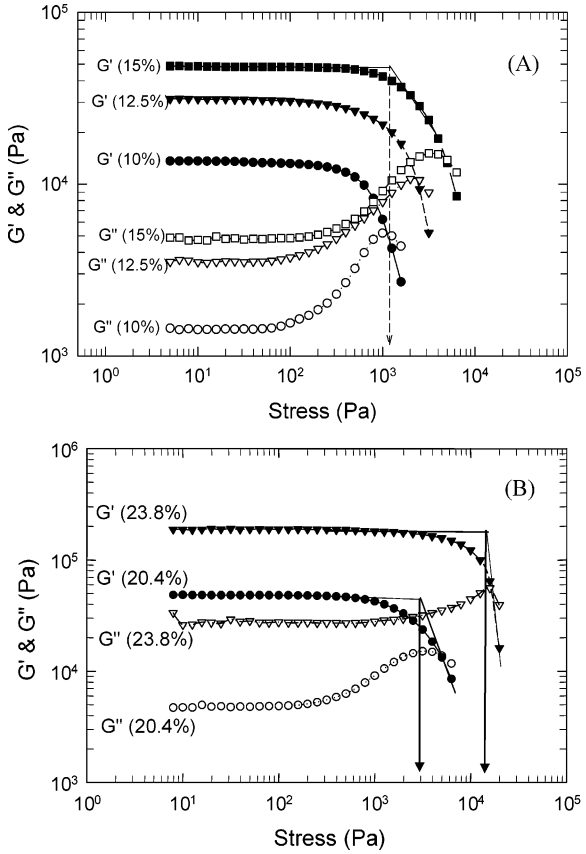

Figure 6. Stress sweep experiments conducted for (A) samples containing different CA concentrations (10, 12.5, and 15 wt %) but the same water content (21.6%) and (B) samples with the same CA concentration (15 wt %) but varying water contents (20.4% and 23.8%). The arrows indicate the yield stress, determined from the onset of the decrease of the elastic (G') moduli.

To pinpoint the sol−gel transition as a function of water content, a multifrequency plot of tan δ (G''/G') as a function of water content for two samples containing 10 and 15 wt % CA was constructed (Figure 5). Determination of the gel point using this method was developed by Winter and Chambon and is appropriately termed as the Winter−Chambon criterion. This procedure has been applied to a variety of polymeric systems.[36−40] The point of intersection of the various curves at different frequencies is indicative of the gel point.[39,40] Data for Figure 5 were obtained from plots similar to that in Figure 2 (dynamic frequency plots) performed at different water contents. For both samples tan δ curves obtained at the different frequencies converge at specific water content. However, unlike conventional gelation, in which these curves diverge after intersecting, our system shows that the curves remain together and are independent of frequency following the convergence. Assuming the initial point of convergence to be the gel point, we find gelation to occur at a slightly lower water content for the more concentrated CA system. Thus, even though increasing water content is the key to inducing the sol−gel properties in our system, polymer concentration also plays a role, albeit minor, in influencing gelation.

Gel Rheology and Microstructure. Figure 6 exhibits the effects of increasing stress amplitude on gel modulus of samples having different CA concentrations and water contents. At low stresses, both G' and G'' are relatively independent of the applied stress, which indicates the materials are in the LVE regime. However, with increasing stress, there is a breakdown of the interactive bonds in the materials and a gradual decrease in G'

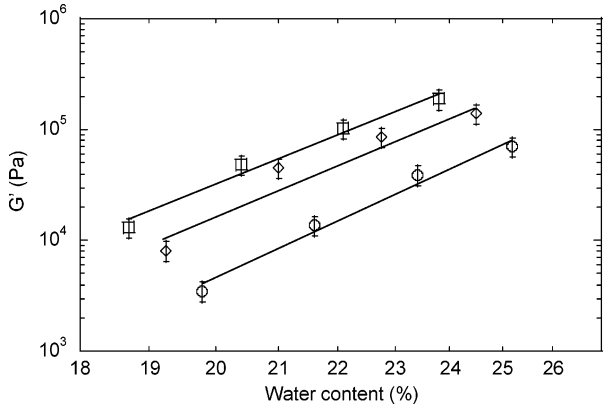

Figure 7. Effect of CA concentration and water content on elastic (G') moduli. CA concentrations: □ 15, ◇ 12.5, and ○ 10 wt % (1 rad s^{-1}).

is observed. Beyond a critical stress value (τ_c), the structure ruptures and/or yields leading to a sharp drop in G'. The yield stress was calculated from the intercept of two asymptotic lines drawn through the initial and postbreakdown G' values (as shown in Figure 6). Several approaches have been described in the literature on measuring the "yield stress" of complex materials,[41] this being one of them. We find from Figure 6 that the yield stress or onset of nonlinearity shifts to higher values with either increasing water content or CA concentration.

Shih et al.[42] have classified gels in terms of strong or weak links based on the onset of nonlinearity in a stress sweep, such as in Figure 6. In strong-linked gels, the links or interactions between flocs of aggregated molecules are stronger than the links within the flocs, and a decrease in the LVE occurs with increasing sample concentration. In the case of weak-linked gels, the intrafloc bonds are more rigid than the interfloc links, failure occurs in the interfloc links, and the limit in linearity increases with concentration. It is evident from Figure 6A that the CA gels are weak-linked as the limit in linearity increases with increasing CA concentration.

It is interesting to note that for all samples shown in Figure 6 G'' shows a maximum at the onset where G' begins to decline. This process may be caused by viscous properties being enhanced as the interfloc bonds break with gradual stress elevation. While more work is being done to elucidate to the mechanism of gel formation, suffice it to say that this type of behavior has been observed in other physical gels.[43]

Figure 7 reveals the effects of water content and CA concentration on the elastic modulus. For all gels investigated G' shifts to higher values with increasing CA concentration and/or water content (Figure 7). Elastic modulus increases substantially, in some cases by an order of magnitude, when the water content or CA concentration is increased. In all cases, G' exhibits a power-law behavior with water content, with the power-law exponent n varying between 10.9−12.5 for 15, 12.5, and 10 wt % CA, respectively. The power-law dependence, together with the similar values for n observed for the various CA concentrations, suggests that the gels' formation mechanism is same in all cases and that they may possess similar microstructures.[44−46]

A direct method for visualizing microstructure is through confocal microscopy.[47] Figure 8 shows the micrographs obtained at different water content for two different CA concentrations. At low CA concentration (10 wt %) and water content (21.6 wt %) an open network is observed (Figure 8A). The observed microstructure seems somewhat aggregated. Increasing the water content to 25.2 wt % appears to enhance the density of the microstructure. Increasing the CA concentration to 15 wt % (Figure 8B) results in a denser network with a fine and more uniform structure.

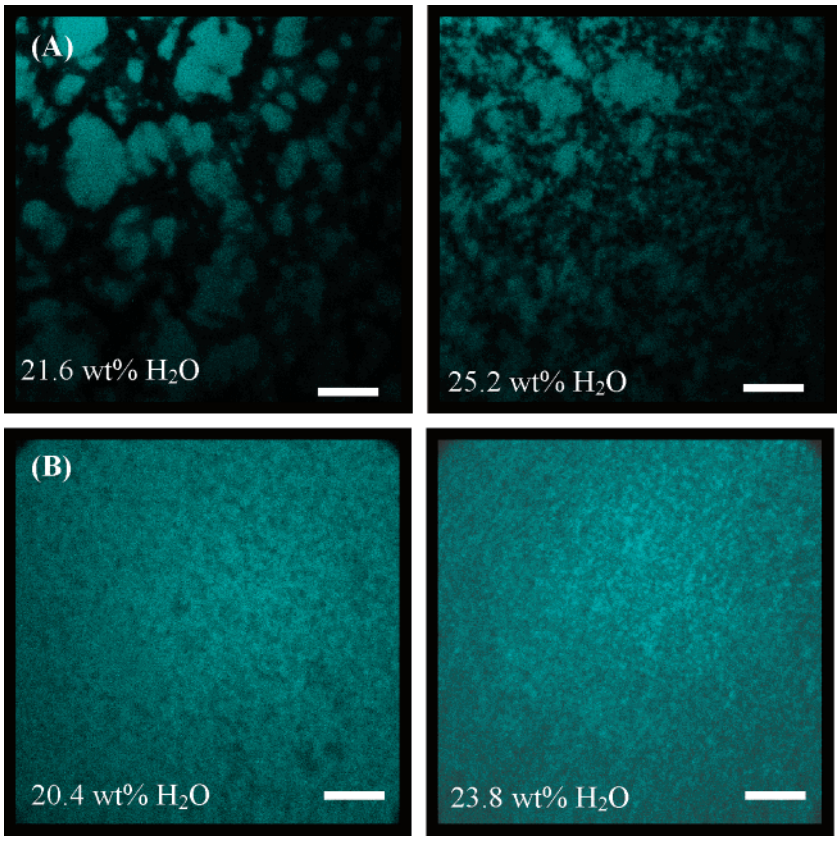

Figure 8. CSLM images for CA concentrations of (A) 10 wt % and (B) 15 wt % at two different water contents.

The fractal dimensions of the gels can be calculated from the images by the box-counting technique using Image J software.[48] In this technique, the fractal dimension can be obtained from the scaling relation $N \propto r^{-D}$, where N is the number of boxes filled with CA, r is the size of the square box, and D is the fractal dimension of the CA network. We find the fractal dimension of the gels obtained via confocal microscopy, regardless of water or CA concentration, to have the same value of $\sim 1.94 \pm 0.04$. Similar values of fractal dimension, independent of polymer concentration, have been reported by Eissa and Khan[48] for a whey protein physical gelling system. In their case, though, the images looked similar and the fractal dimension was corroborated independently from rheology. Pugnaloni et al., on the other hand, have obtained results very similar to ours for caseinate gels.[49] These gels exhibit visually different structures, ranging from open to dense and more uniform, yet with all having the same calculated fractal dimension from image analysis. They suggest that fractal dimension alone may not always be sensitive enough to capture the differences observed in gel microstructure.

Conclusions

The effect of water addition on a CA/DMA system was investigated using steady-state and dynamic rheology. The addition of water led to enhanced steady shear viscosity and dynamic elastic modulus, with the system losing clarity and ultimately turning into an opaque self-supporting gel. The sol−gel transition was dependent on CA concentration with gel formation occurring at slightly lower water content with higher CA concentration. The changes in the elastic modulus during gelation correlated well with the combined solubility parameter (δ) and, in particular, the Hansen hydrogen-bonding solubility parameter index (δ_h) of the solvent system, suggesting hydrogen-bonding interactions may be the major route initiating the sol−gel process.

For all gels studied, the elastic modulus and the critical stress to yield shifted to higher values with increasing CA concentration and/or water content. Such increase in critical stress with polymer concentration indicates our gels to be "weak-linked" in which the interfloc linkages are weaker than the intrafloc links. In addition, the elastic modulus exhibited a power-law behavior with water content; the power-law exponent was found to be independent of the CA concentration of the gel suggesting that the mechanism of gel formation upon water addition to be independent of polymer concentration. Finally, confocal microcopy was used to directly probe the gel microstructure for systems containing two CA concentrations. We found that addition of water led to formation of a denser gel network and that the gels had a more open microstructure at the lower CA concentration.

Acknowledgment. The authors gratefully acknowledge the United States Department of Agriculture (USDA-NRI 2000-01864) for financial support.

References and Notes

(1) Kadla, J. F.; Gilbert, R. D. Cellulose structure: a review. *Cellul. Chem. Technol.* **2000**, *34*, 197−216.
(2) Saalwachter, K.; Burchard, W. Cellulose in new metal-complexing solvents. 2. Semidilute behavior in Cd-tren. *Macromolecules* **2001**, *34*, 5587−5598.
(3) Hattori, K.; Cuculo, J. A.; Hudson, S. M. New solvents for cellulose: hydrazine/thiocyanate salt system. *J. Polym. Sci., Part A: Polym. Chem.* **2002**, *40*, 601−611.
(4) Tsunashima, Y.; Hattori, K. Substituent distribution in cellulose acetate: its control and the effect on structure formation in solution. *J. Colloid Interface Sci.* **2000**, *228*, 279−286.
(5) Gross, R. A.; Scholz, C. *Biopolymers from Polysaccharides and Agroproteins*; Oxford University Press, 2001.
(6) Kawanishi, H.; Tsunashima, Y.; Okada, S.; Horii, F. Change in chain stiffness in viscometric and ultracentrifugal fields: cellulose diacetate in *N,N*-dimethylacetamide dilute solution. *J. Chem. Phys.* **1998**, *108* (14), 6014−6025.
(7) Tsunashima, Y.; Kawanishi, H.; Horii, F. Reorganization of dynamic self-assemblies of cellulose diacetate in solution: dynamical critical-like fluctuations in lower critical solution temperature system. *Biomacromolecules* **2002**, *3*, 1276−1285.
(8) Kawanishi, H.; Tsunashima, Y.; Horii, F. Dynamic light scattering study of structural changes of cellulose diacetate in solution under couette flow. *Macromolecules* **2000**, *33*, 2092−2097.
(9) Wee, W.-K.; Mackley, M. R. The rheology and processing of a concentrated cellulose acetate solution. *Chem. Eng. Sci.* **1998**, *53*, 1131−1144.
(10) Tweddle, T. A.; Sourirajan, S. Effect of ethanol−water mixture as gelation medium during formation of cellulose acetate reverse osmosis membranes. *J. Appl. Polym. Sci.* **1978**, *22*, 2265−2274.
(11) Hoernschemeyer, D. The influence of solvent type on the viscosity of concentrated polymer solutions. *J. Appl. Polym. Sci.* **1974**, *18*, 61−75.
(12) Pintraric, B.; Rogosic, M.; Mencer, H. J. Dilute solution properties of cellulose diacetate in mixed solvents. *J. Mol. Liq.* **2000**, *85*, 331−350.
(13) Gomez-Bujedo, S.; Fleury, E.; Vignon, M. R. Preparation of cellouronic acids and partially acetylated cellournic acids by TEMPO/NaClO oxidation of water-soluble cellulose acetate. *Biomacromolecules* **2004**, *5*, 565−571.
(14) Bochek, A. M.; Kalyuzhnaya, L. M. Interaction of water with cellulose and cellulose acetates as influenced by the hydrogen bond system and hydrophilic−hydrophobic balance of the macromolecules. *Macromol. Chem. Polym. Mater.* **2002**, *75*, 989−993.
(15) Kesting, R. E.; Barsh, M. K.; Vincent, A. L. Semipermeable membranes of cellulose acetate for desalination in the process of reverse osmosis II. Parameters affecting membrane gel structure. *J. Appl. Polym. Sci.* **1965**, *9*, 1873−1893.
(16) Pilon, R.; Kunst, B.; Sourirajan, S. Studies on the development of improved reverse osmosis membranes from cellulose acetate−acetone−formamide casting solution. *J. Appl. Polym. Sci.* **1971**, *15*, 1317−1334.
(17) Khalil, S. A. Phase separation of cellulose derivatives: effects of polymer viscosity and dielectric constant of nonsolvent. *J. Pharm. Sci.* **1973**, *62*, 1883−1884.
(18) Vogrin, N.; Stropnik, C.; Musil, V.; Brumen, M. The wet phase separation: the effect of cast solution thickness on the appearance of macrovoids in the membrane forming ternary cellulose acetate/acetone/water system. *J. Membr. Sci.* **2002**, *207*, 139−141.
(19) Kunst, B.; Sourirajan, S. Evaporation rate and equilibrium phase separation data in relation to casting conditions and performance of porous cellulose acetate reverse osmosis membranes. *J. Appl. Polym. Sci.* **1970**, *14*, 1983−1996.
(20) Matsuyama, H.; Nishiguchi, M.; Kitamura, Y. Phase separation mechanism during membrane formation by dry-cast process. *J. Appl. Polym. Sci.* **2000**, *77*, 776−782.
(21) Vaessen, D. M.; McCormick, A. V.; Francis, L. F. Effect of phase separation on stress development in polymeric coatings. *Polymer* **2002**, *43*, 2267−2277.
(22) Reuvers, A. J.; Altena, F. W.; Smolders, C. A. Demixing and gelation behavior of ternary cellulose acetate solutions. *J. Polym. Sci., Part B: Polym. Phys.* **1986**, *24*, 793−804.
(23) Hao, J. H.; Wang, S. Calculation of alcohol−acetone−cellulose acetate ternary phase diagram and their relevance to membrane formation. *J. Appl. Polym. Sci.* **2001**, *80*, 1650−1657.
(24) Iiyina, E.; Daragan, V. Self-diffusion of dimethyl sulfoxide and dimethylformamide in solutions and gels of cellulose acetates by pulsed field gradient NMR. *Macromolecules* **1994**, *27*, 3759−3763.
(25) Alie, C.; Pirard, R.; Pirard, J-P. Preparation of low-density xerogels from mixtures of TEOS with substituted alkoxysilanes. II. Viscosity study of the sol−gel transition. *J. Non-Cryst. Solids* **2003**, *320*, 31−39.

(26) Lizaso, E.; Munoz, M. E.; Santamaria, A. Formation of gels in ethylcellulose solutions. An interpretation from dynamic viscoelastic results. *Macromolecules* **1999**, *32*, 1883−1889.
(27) Maestro, A.; Gonzalez, C.; Gutierrez, J. M. Shear thinning and thixotropy of HMHEC and HEC water solutions. *J. Rheol.* **2002**, *46*, 1445−1457.
(28) Eissa, A. S.; Bisram, S.; Khan, S. A. Polymerization and gelation of whey protein isolates at low pH using transglutaminase enzyme. *J. Agric. Food Chem.* **2004**, *52*, 4456−4464.
(29) Fuji, S.; Sasaki, N.; Nakata, M. Rheological studies on the phase separation of hydroxylpropylcellulose solution systems. *J. Polym. Sci., Part B: Polym. Phys.* **2001**, *39*, 1976−1986.
(30) Pai, V.; Srinivasarao, M.; Khan, S. A. Evolution of microstructure and rheology in mixed polysaccharide systems. *Macromolecules* **2002**, *35*, 1699−1707.
(31) Raghavan, S. R.; Walls, H. J.; Khan, S. A. Rheology of silica dispersions in organic liquids: new evidence for solvation forces dictated by hydrogen bonding. *Langmuir* **2000**, *16* (21), 7920−7930.
(32) Lazaridou, A.; Biliaderis, C. G.; Izydorczyk, M. S. Molecular size effects on rheological properties of oat β-glucans in solution and gels. *Food Hydrocolloids* **2003**, *17*, 693−712.
(33) Griswold, P. D.; Cuculo, J. A. An experimental study of the relationship between rheological properties and spinnability in the dry spinning of cellulose acetate−acetone solutions. *J. Appl. Polym. Sci.* **1974**, *18*, 2887−2902.
(34) Grulke, E. A. Solubilty Parameter Values. In *Polymer Handbook*, 4th ed.; Brandrup, J., Immergut, E. H., Grulke, E. A., Eds.; John Wiley & Sons Inc.: New York, 1999; pp VII 675−714.
(35) Hansen, C. M. The universality of the solubility parameter. *Ind. Eng. Chem. Prod. Res. Dev.* **1969**, *8* (1), 2−11.
(36) Dumitras, M.; Friedrich, C. Network formation and elasticity evolution on dibenzylidene sorbitol/poly(propylene oxide) physical gels. *J. Rheol.* **2004**, *48* (5), 1135−1146.
(37) Cossar, S.; Nichetti, D.; Grizzuti, N. A rheological study of the phase transition in thermoplastic polyurethanes. Critical gel behavior and microstructure development. *J. Rheol.* **2004**, *48* (3), 691−703.
(38) Power, D. J.; Rodd, A. B.; Paterson, L.; Boger, D. V. Gel transition studies on nonideal polymer networks using small amplitude oscillatory rheometry. *J. Rheol.* **2004**, *42* (5), 1021−1036.
(39) Fahrlander, M.; Fuchs, K.; Mulhaupt, R.; Friedrich, C. Linear and nonlinear rheological properties of self-assembling tectons in polypropylene matrices. *Macromolecules* **2003**, *36*, 3749−3457.
(40) Chiou, B-S.; Raghavan, S. R.; Khan, S. A. Effect of colloidal fillers on the cross-linking of a UV-curable polymer: gel point rheology and the Winter−Chambon criterion. *Macromolecules* **2001**, *34*, 4526−4533.
(41) Walls, H. J.; Caines, S. B.; Sanchez, A. M.; Khan, S. A. Yield stress and wall slip phenomena in colloidal silica gels. *J. Rheol*. **2003**, *47*, 847−868.
(42) Shih, W. H.; Shih, W. Y.; Kim, S. I.; Liu, J.; Aksay, I. A. Scaling behavior of the elastic properties of colloidal gels. *Phys. Rev. A* **1990**, *42*, 4772−4780.
(43) Sim, H. G.; Ahn, K. H.; Lee, S. J. Large amplitude oscillatory shear behavior of complex fluids investigated by a network model: a guideline for classification. *J. Non-Newtonian Fluid Mech.* **2003**, *112*, 237−250.
(44) Khan, S. A.; Zoeller, N. Dynamic rheological behavior of flocculated fumed silica suspensions. *J. Rheol.* **1993**, *37*, 1225−1235.
(45) Buscall, R.; Mills, P. D. A.; Goodwin, J. W.; Lawson, D. W. Scaling behavior of the rheology of aggregate networks formed from colloidal particles. *J. Chem. Soc., Faraday Trans. 1* **1988**, *48*, 4249−4260.
(46) Shay, J. S.; Raghavan, S. R.; Khan, S. A. Thermoreversible gelation in aqueous dispersions of colloidal particles bearing grafted poly(ethylene oxide) chains. *J. Rheol* **2001**, *45*, 913−918.
(47) Hagiwara, T.; Kumagai, H.; Matsunaga, T.; Nakamura, K. Analysis of aggregate structure in food protein gels with the concept of fractal. *Biosci., Biotechnol., Biochem.* **1997**, *61*, 11663−11667.
(48) Eissa, A. S.; Khan, S. A. Acid-induced gelation of enzymatically modified, preheated whey proteins. *J. Agric. Food Chem.* **2005**, *53*, 5010−5017.
(49) Pugnaloni, L. A.; Matia-Merino, L.; Dickinson, E. Microstructure of acid-induced caseinate gels containing sucrose: quantification from confocal microscopy and image analysis. *Colloids Surf., B* **2005**, *42*, 211−217.

BM0611681